Aerodynamic performance due to forewing and hindwing interaction in gliding dragonfly flight

Jie Zhang and Xi-Yun Lu*

Department of Modern Mechanics, University of Science and Technology of China, Anhui, Hefei 230026, China

(Received 14 April 2009; revised manuscript received 1 June 2009; published 22 July 2009)

Aerodynamic performance due to forewing and hindwing interaction in gliding dragonfly flight has been studied using a multiblock lattice Boltzmann method. We find that the interactions between forewing and hindwing effectively enhance the total lift force and reduce the drag force on the wings compared to two independent wings. The interaction mechanism may be associated with the triangular camber effect by modulating the relative arrangement of the forewing and hindwing. The results obtained in this Brief Report provide physical insight into the understanding of aerodynamic behaviors for gliding dragonfly flight.

DOI: 10.1103/PhysRevE.80.017302 PACS number(s): 47.63.−b, 47.32.C−, 47.32.Ff, 47.85.L−

Dragonflies glide as part of their natural flight repertoire, and they benefit from the lower cost of gliding compared with flapping flight [1]. Gliding may aid dragonflies' thermoregulation [2] by allowing them to use convective cooling as they move through the air, without the heat produced during gliding by the thoracic flight muscles [3]. The aerodynamic aspect in the gliding flight is also an important issue. Complex flow phenomena induced by the interactions between forewings and hindwings in gliding have never been studied but are highly desirable for understanding the aerodynamic behaviors.

Dragonflies are four-winged insects and a distinct feature of dragonfly flight is the interactions of the flow over forewings and hindwings. Investigations have previously been made on how such interactions affect the aerodynamic performance for flapping dragonfly flight [4–7]. The forces acting on the gliding dragonfly *Sympetrum sanguineum* were obtained by analyzing the filmed free gliding flight of the dragonfly [1]. The lift and drag were also measured from the isolated wings of dragonflies [1] and artificial wing models [8]. However, it has been found that the sum of the lift on each isolated wing of a dragonfly is insufficient to balance its weight for the angles of attack adopted in its gliding, suggesting the crucial importance of the interactions between forewing and hindwing flows. As the Reynolds number for the gliding wings is $O(10^3)$, it is speculated that quasisteady analysis may fail to predict sufficient lift required for gliding and to capture the key physics of the interactions. This recognition motivated our present numerical experiment to study the interactions between forewing and hindwing and to reveal the unsteady aerodynamic mechanisms for the gliding flight.

Given the complexity and expensive cost in three-dimensional (3D) computations of flow over a pleated plate, like that over a real dragonfly wing [6,9], it is natural to ask if a two-dimensional (2D) computation on a simpler sectional profile (e.g., a flat plate) may still clarify certain mechanisms in insect flights. Interestingly, two counteracting effects in dragonfly wing modeling have been documented. On the one hand, there is evidence that the computed averaged lift on a 2D flat plate may be higher than its 3D counterpart by about 20% [6]. On the other hand, measurements and computations have revealed that the lift and the lift/drag ratio on a 2D pleated plate are higher than those on a 2D flat plate by about 15% and 30%, respectively [10,11]. Therefore, it is possible to achieve a reasonable estimate of the forces on the dragonfly wings in gliding flight by a 2D flat plate model; additional 3D and pleated effects for understanding the lift behavior are refinements rather than necessities.

This being the case, in our study a 2D virtual model shown in Fig. 1 is used, and the forewing and hindwing are mimicked by 2D flat plates [7] with the chord lengths c_1 and c_2 and the angles of attack α_1 and α_2.

To set the computational parameters realistically, we analyzed our measured data of free-flight dragonfly in laboratory using projected comb fringe method and specifically picked the gliding flight mode to obtain the data for both forewings and hindwings. We also employed the filmed free gliding flight of dragonfly *S. sanguineum* [1] to select the parameters. Based on experimental evidence, the mean chord length $c=0.5(c_1+c_2)$ is about 0.85 cm, the gliding speed is at $U=2$ m/s, and the Reynolds number is $\mathrm{Re}=cU/\nu\simeq 1000$. Here the kinematic viscosity and air density at temperature of 32 °C, $\nu=1.66\times10^{-5}$ m^2/s and $\rho=1.13$ kg/m^3, respectively, are used. Experimental data also show that generically $c_1<c_2$ and in gliding flights $\alpha_1<\alpha_2$. Therefore, we carried out a systematic study for $0°\leq\alpha_1\leq6°$ and $6°\leq\alpha_2\leq14°$, with the chord ratios being both $c_1/c_2=0.9/1.1$ and 1/1. Moreover, in accordance with the experimental data, the ranges of the vertical and horizontal distances of the forewing trailing edge and hindwing leading edge, i.e., H and G

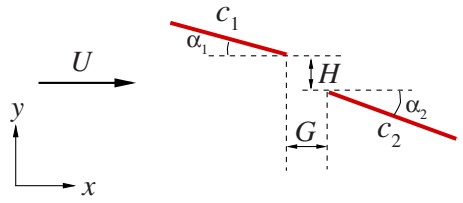

FIG. 1. (Color online) Sketch of the relative arrangement of forewing [the red (left) line] and hindwing [the red (right) line]. Cartesian coordinate system (x,y) with the origin at the leading edge of forewing is used.

*Author to whom correspondence should be addressed. FAX: +86-551-3606459. xlu@ustc.edu.cn

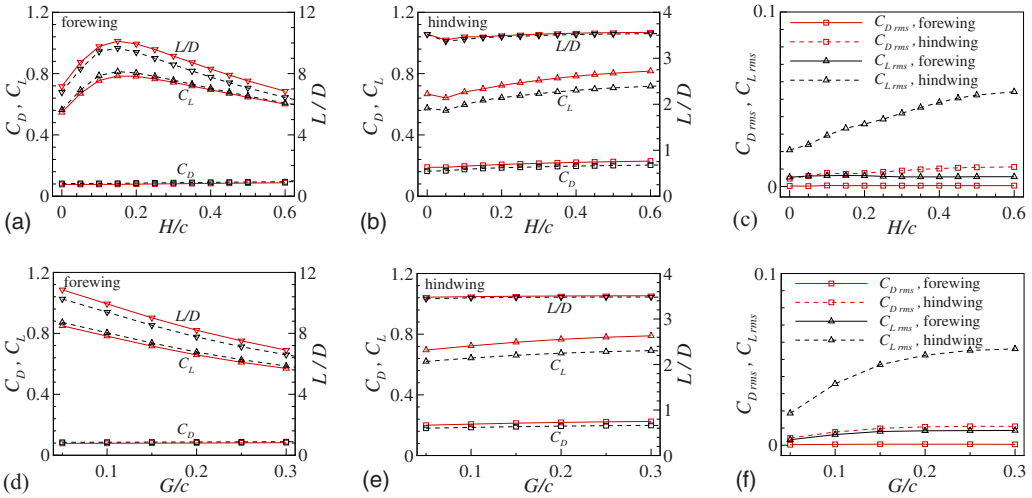

FIG. 2. (Color online) Time-averaged lift (C_L) and drag (C_D) coefficient and their ratio (L/D) for $\alpha_1=2°$, $\alpha_2=12°$, and Re=1000. (a) Forewing at $G/c=0.1$. (b) Hindwing at $G/c=0.1$. The red and black symbols represent C_L (△), C_D (□), and L/D (▽). The solid red and dashed black lines denote $c_1/c_2=0.9/1.1$ and 1/1. (c) Root-mean-square (rms) values of the fluctuations of C_L^* and C_D^* on the forewing and hindwing at $G/c=0.1$ and $c_1/c_2=0.9/1.1$. (d) Forewing at $H/c=0.2$. (e) Hindwing at $H/c=0.2$. (f) rms values of the fluctuations of C_L^* and C_D^* for $H/c=0.2$. The lines and symbols in (d)–(f) have the same meanings in (a)–(c), respectively.

(Fig. 1), were set as $0\le H\le 0.6c$ and $0.05c\le G\le 0.3c$.

We performed a direct numerical simulation using a multiblock lattice Boltzmann method [12,13] with second-order accurate treatment for the boundary conditions [14]. Based on our extensive tests, the computational domain was chosen as $-10c\le x\le 30c$ and $-20c\le y\le 20c$ with the finest lattice spacing of $0.005c$ in the near region of the wings. Our code has carefully been validated [15–17], and the computed results have been confirmed to be independent of the lattice spacing and computational domain size. The computed time elapses to $1000c/U$. The instantaneous lift and drag coefficients are defined as $C_L^*=L^*/(0.5\rho U^2 c)$ and $C_D^*=D^*/(0.5\rho U^2 c)$, respectively, where L^* and D^* are the lift and drag forces by integrating the viscous stress and pressure over the wing. Time-averaged lift and drag coefficients, denoted as C_L and C_D with the corresponding forces L and D, were calculated after careful elimination of the transient part in their time-dependent variations.

The computed forces on both the forewing and hindwing are shown in Figs. 2 and 3 for various values of (H,G) and (α_1,α_2), respectively. Observe Fig. 2 and focus on the drag first. The C_D versus H or G is nearly constant for the forewing [Figs. 2(a) and 2(d)] but slightly increases for the hindwing [Figs. 2(b) and 2(e)]. To examine the effect of the forewing/hindwing flow interactions on the forces, the time-averaged lift and drag coefficients on the two isolated wings, C_L^i and C_D^i, are also calculated and given in Table I. The interactions obviously reduce the drag on each wing compared to their isolated counterparts; this fact is well verified by the calculated cases in the range of given parameters. As a typical case listed in Table I, the drag reductions relative to the isolated wings are 18.6% for the forewing and 21.6% for the hindwing. In addition, for tandem bodies moving through a fluid, it has been known that if the bodies are rigid the downstream one will generally experience a drag reduction, while if the bodies are flexible the leader will bear a drag reduction but the follower will suffer a drag increase [18]. Correspondingly, the present findings provide a different understanding of the dynamic behaviors of body interaction and prove that a dragonfly may smartly adopt the relative arrangement of its forewings and hindwings in gliding flight to obtain a drag reduction on each wing.

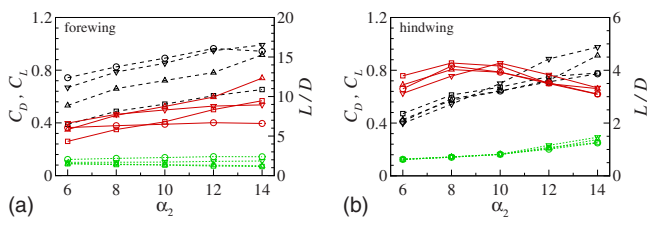

FIG. 3. (Color online) Time-averaged lift (C_L) and drag (C_D) coefficient and their ratio (L/D) for $H/c=0.2$, $G/c=0.1$, $c_1/c_2=0.9/1.1$, and Re=1000: (a) forewing; (b) hindwing. The lines represent C_L (dashed black lines), C_D (dotted green lines), and L/D (red solid lines) and the color symbols $\alpha_1=0°$ (□), 2° (△), 4° (▽), and 6° (○).

Regarding the variation in the lift and lift/drag ratio with (H,G), both C_L and L/D curves of the forewing reach a peak at $H/c=0.16$ but decrease monotonically with G [Figs. 2(a) and 2(d)]. Then, the C_L and L/D on the hindwing increase with H or G [Figs. 2(b) and 2(e)]. Compared to the isolated wings in Table I, the C_L and L/D on the forewing are significantly enhanced: in Table I, $C_L\simeq 4.655C_L^i$ and $L/D\simeq 5.715(L^i/D^i)$. The higher lift on the forewing is helpful in flight stability [19]. In contrast, the hindwing suffers a lift reduction relative to the isolated wing; say the C_L reduction by 25.4% and the L/D reduction by 3.75% in Table I. Consequently, the overall effect of the interactions on the total aerodynamic forces (the sum of the forces on both the forewing and hindwing) is still very beneficial: a reduction in total drag (such as 20.8% in Table I) and an enhancement of the total lift (33.7%) or the total L/D (68.7%).

In addition, for the influence of the chord ratio on the

TABLE I. Comparison of the forces for the forewing/hindwing interaction and the corresponding isolated wing case at $\alpha_1=2°$, $\alpha_2=12°$, $c_1/c_2=0.9/1.1$, $H/c=0.2$, and $G/c=0.1$. The superscript i denotes the isolated wing.

	C_D	C_L	L/D	C_D^i	C_L^i	L^i/D^i
Forewing	0.079	0.782	9.899	0.097	0.168	1.732
Hindwing	0.207	0.723	3.493	0.264	0.958	3.629
Total	0.286	1.505	5.262	0.361	1.126	3.119

forces for $c_1/c_2=0.9/1.1$ and 1/1, Fig. 2 indicates that the ratio of 0.9/1.1 somewhat improves the L/D of the forewing and the C_L of the hindwing compared to the ratio of 1/1.

The force fluctuations on both the wings are shown in Figs. 2(c) and 2(f). Especially on the forewing, the fluctuations are suppressed compared to isolated wings though the lift fluctuation on the hindwing is stronger due to vortex shedding to be shown below. The forewing/hindwing interactions reduce the overall force fluctuations and thus the body oscillation, which is desirable for gliding.

Figure 3 shows the forces on the forewing and hindwing versus α_1 and α_2. A careful inspection indicates that the C_D on the forewing in Fig. 3(a) increases with α_1 for fixed α_2 and somewhat decreases with α_2 for $\alpha_1=0°$ and 2°, but it remains nearly unchanged for $\alpha_1=4°$ and 6°. The C_L increases monotonically with α_2 for $\alpha_1=0°-4°$, while at higher α_1, such as 6°, the C_L increases with α_2 and then decreases with further increase in α_2. The L/D in most cases is greater than 5 and even reaches 12.4 at $\alpha_1=2°$ and $\alpha_2=14°$. Moreover, the C_L and C_D on the hindwing in Fig. 3(b) increase with α_2 as expected and the L/D reaches a higher value about 4.5 during $\alpha_2=8°-10°$. A synthetical analysis of the total forces and their fluctuations based on our computed results tells that the ranges of α_1 and α_2 with favorable aerodynamic performance are $\alpha_1=2°-4°$ and $\alpha_2=10°-14°$, respectively. This is consistent with the preceding observations of gliding dragonfly flight.

We can now answer the question whether the lift generated by the wings is enough to balance the weight of a typical dragonfly by using the morphologic data of the gliding dragonfly *S. sanguineum* [1] for our selected parameters. The mean quantities by five specimens of the same species are forewing area of 332 mm^2, hindwing area of 448 mm^2, and mass of 125 mg or weight of 1.225×10^{-3} N. As a typical case in Table I, the total lift on all four wings (neglecting the body) is 1.323×10^{-3} N, which is larger than the weight. This is not just fortuitous; we have identified that most calculated cases shown above can provide enough lift for supporting dragonflies gliding. Recall that the sum of the lifts on isolated wings cannot balance the weight for the angles of attack adopted by dragonfly gliding, as has been found by wind-tunnel measurements [1]; this interaction effect is of crucial significance in dragonfly gliding flight.

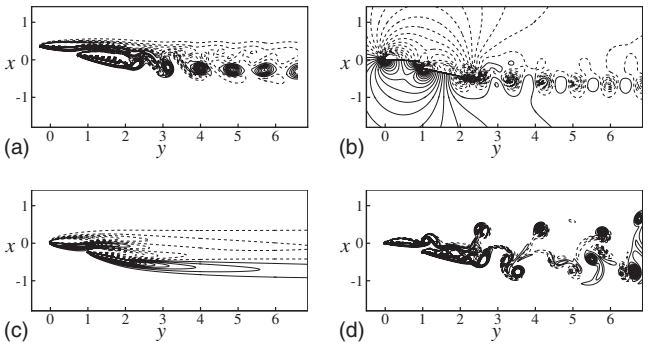

FIG. 4. Instantaneous flow structures for $H/c=0.2$, $G/c=0.1$, $\alpha_1=2°$, $\alpha_1=12°$, and $c_1/c_2=0.9/1.1$: (a) vorticity at Re=1000; (b) relative pressure with respect to the incoming flow pressure at Re=1000; (c) vorticity at Re=300; and (d) vorticity at Re=2000. Solid and dashed lines represent positive and negative values, respectively.

The above critical favorable effect of the interactions between forewing and hindwing can be physically understood by examining the flow structures around the wings. Figure 4(a) shows a snapshot of vortical structure for the case in Table I. The organized vortex shedding into the wake indicates that the flow is inherently unsteady. As the pressure force dominates the viscous stress, we plot the corresponding pressure field around both the wings in Fig. 4(b), which shows clearly the high and low pressure levels on the lower and upper sides of the wings as required for an effective lift generation. Then, we can reasonably view the flow passed both the wings as a single flow system in which the forewing and hindwing at $\alpha_1<\alpha_2$ form a slotted camber wing or "triangular camber" [8]. Thus, similar to the high-lift control device by means of airfoil and its trailing flap in civil aircraft landing [20], the triangular camber effect is generated by fluid-mediated interactions for flow passed both the wings in a relative arrangement adopted by dragonfly gliding (Fig. 1), which can effectively enhance the lift and the lift/drag ratio. This triangular camber effect in improving the aerodynamic characteristics was also confirmed by wing-tunnel measurement of the forces on Λ-shape models for mimicking the togetherness of forewing and hindwing in dragonfly gliding [8].

We finally examine the Reynolds number dependence of the flows and forces and compare three cases, Re=300, 1000, and 2000, shown in Fig. 4 for the vortical structures. The detailed vortex structures at the three Reynolds numbers are markedly different, with quasisteady vortex evolution at Re=300 [Fig. 4(c)] and complex finer structures at Re=2000 [Fig. 4(d)]. The lift on the wings increases with Re as expected, say $C_L=0.770$ on the forewing and 0.701 on the hindwing at Re=300 and the counterparts 0.949 and 0.791 at Re=2000. The aerodynamic behaviors at Re=300 and 2000 are qualitatively similar to those at Re=1000 described above. We thus assert that the forewing/hindwing interac-

tions improve the aerodynamic performance in gliding dragonfly flight for $\mathrm{Re} \sim O(10^2)$–$O(10^3)$.

In summary, the aerodynamic performance in gliding dragonfly flight has been systematically studied. We have revealed that the forewing/hindwing interactions can enhance the total lift force effectively and reduce the drag force on the wings compared to two isolated wings. The results obtained in this Brief Report provide physical insight into the understanding of aerodynamic behaviors for gliding dragonfly flight.

We are grateful to Professor J.-Z. Wu for his kind help in improving this Brief Report. This work was supported by the Innovation Project of the Chinese Academy of Sciences (Grant No. KJCX2-YW-L05) and the National Natural Science Foundation of China (Grant No. 10832010).

[1] J. M. Wakeling and C. P. Ellington, J. Exp. Biol. **200**, 557 (1997).
[2] B. Heinrich, *The Hot-Blooded Insects: Strategies and Mechanisms of Thermoregulation* (Harvard University Press, Cambridge, 1993).
[3] M. L. May, Ecol. Monogr. **46**, 1 (1976).
[4] R. A. Norberg, in *Swimming and Flying in Nature*, edited by T. Y. Wu, C. J. Brokaw, and C. Brennen (Plenum, New York, 1975), Vol. 2, pp. 763–780.
[5] C. Somps and M. W. Luttges, Science **228**, 1326 (1985).
[6] M. Sun and S. Lan, J. Exp. Biol. **207**, 1887 (2004).
[7] Z. J. Wang and D. Russell, Phys. Rev. Lett. **99**, 148101 (2007).
[8] M. Okamoto, K. Yasuda, and A. Azuma, J. Exp. Biol. **199**, 281 (1996).
[9] H. Liu and K. Kawachi, J. Comput. Phys. **146**, 124 (1998).
[10] A. B. Kesel, J. Exp. Biol. **203**, 3125 (2000).
[11] A. Vargas, R. Mittal, and H. Dong, Bioinspir. Biomim. **3**, 026004 (2008).
[12] D. Yu, R. Mei, and W. Shyy, Int. J. Numer. Methods Fluids **39**, 99 (2002).
[13] Y. Peng, C. Shu, Y. T. Chew, X. D. Niu, and X.-Y. Lu, J. Comput. Phys. **218**, 460 (2006).
[14] P. Lallemand and L. S. Luo, J. Comput. Phys. **184**, 406 (2003).
[15] T. Gao, Y.-H. Tseng, and X.-Y. Lu, Int. J. Numer. Methods Fluids **55**, 1189 (2007).
[16] T. Gao and X.-Y. Lu, Phys. Fluids **20**, 087101 (2008).
[17] J. Zhang, N. S. Liu, and X.-Y. Lu, Phys. Rev. E **79**, 045306(R) (2009).
[18] L. Ristroph and J. Zhang, Phys. Rev. Lett. **101**, 194502 (2008).
[19] R. Nelson, *Flight Stability and Automatic Control* (McGraw-Hill, New York, 1989).
[20] J. W. van der Burg, J. E. J. Maseland, and F. J. Brandsma, Aerosp. Sci. Technol. **8**, 389 (2004).